



De Luca, F., & Lombardi, L. (2017). EC8 design through linear time history analysis versus response spectrum analysis - is it an enhancement for PBEE? In *16th World Conference on Earthquake Engineering, 16WCEE 2017, Santiago, Chile* Article 1155 National Information Centre for Earthquake Engineering (NICEE).  
<http://www.nicee.org/wcee/index2.php>

Peer reviewed version

[Link to publication record on the Bristol Research Portal](#)  
PDF-document

This is the author accepted manuscript (AAM). The final published version (version of record) is available online via NICEE at <http://www.nicee.org/wcee/index2.php>. Please refer to any applicable terms of use of the publisher.

## University of Bristol – Bristol Research Portal

### General rights

This document is made available in accordance with publisher policies. Please cite only the published version using the reference above. Full terms of use are available:  
<http://www.bristol.ac.uk/red/research-policy/pure/user-guides/brp-terms/>



## EC8 DESIGN THROUGH LINEAR TIME HISTORY ANALYSIS VERSUS RESPONSE SPECTRUM ANALYSIS – IS IT AN ENHANCEMENT FOR PBEE?

F. De Luca<sup>(1)</sup>, L. Lombardi<sup>(2)</sup>

<sup>(1)</sup> Lecturer in Civil Engineering, University of Bristol, [flavia.deluca@bristol.ac.uk](mailto:flavia.deluca@bristol.ac.uk)

<sup>(2)</sup> Ph.D. Student in Civil Engineering, University of Bristol, [luca.lombardi@bristol.ac.uk](mailto:luca.lombardi@bristol.ac.uk)

### **Abstract**

Eurocode 8-conforming design of a 12-storey Reinforced Concrete building is carried out through Response Spectrum Analysis (RSA) and Linear Time History Analysis (LTHA). RSA is the reference design method; it accounts for higher modes effects through an approximate combination of modal results, and the input is characterized by a smoothed response spectrum. On the other hand, assessment of structures in the Performance Based Earthquake Engineering framework is primarily carried through Nonlinear Time-History Analysis, selecting sets of accelerograms. LTHA as design methodology allows direct comparison of linear and nonlinear response between design and assessment phases with the same set of accelerograms. This approach decouples the linear-nonlinear modelling problem from the spectrum-accelerogram input selection problem. This preliminary study investigates whether the Eurocode 8-design process is affected by the change in the linear analysis methodology; i.e., LTHA in lieu of RSA, and how the force-based design should be implemented when using LTHA. Two 12-storey RC archetype buildings are designed for different ductility classes. Spectrum-compatible accelerograms provide conservative results and similar design outcome for RSA and LTHA. Moreover, the high variability of LTHA results can be an issue since Eurocode 8-record selection does not provide restraints on the standard deviation of the input. LTHA has also a great potential as methodology for the assessment of approximate fragility curves for intermediate level of damage (excluding collapse), serviceability limit states and for bespoke analyses for near source conditions. The target is to come up with a robust methodological procedure both force-based and displacement-based to promote this method as option in future versions of Eurocode 8.

*Keywords: Linear Time-History Analysis, Response Spectrum Analysis, EC8 Design, RC Moment Resisting Frame*



## 1. Introduction

Design of structures in seismic prone countries (e.g., according to Eurocode 8 [1]) is made through linear Response Spectrum Analysis (RSA). RSA is an approximate approach for the evaluation of linear dynamic response of structures. It employs results of static analyses (for each considered mode of vibration) combined on the basis of modal properties of structures, in order to calculate the peak value of the response. The mode combination is the most critical aspect of such analysis approach. Several combination rules of modal response peak values were proposed in the last century [2, 3]. The Complete Quadratic Combination (CQC), which derives from the principles of Stochastic Mechanics, is the combination rule for RSA since 1980s [4], although it presents some limits for unusually stiff buildings such as nuclear power plants [5], near source impulsive earthquakes and higher mode dominated structures [6]. An innovative method for the evaluation of seismic response by modal superposition using correlation coefficient and peak factors consistent with the power spectral density and duration of seismic excitation is proposed by [7]. However, the main reason for RSA in lieu of proper Linear Time-History Analysis (LTHA) is that the latter requires selection and availability of accelerograms, and it can be time-consuming. On the other hand, in the last decades, earthquake engineering has progressed significantly on the selection of accelerograms and computational power of computers has improved significantly. Based on the previous considerations, LTHA may be also a useful methodology for simplified-Performance Based Earthquake Engineering (PBEE) assessment framework. As an example, reasonably accurate fragility curves for serviceability limit states can be obtained through this analysis and they can provide information at the early stage design of a structure.

LTHA is proposed, herein, as an alternative linear methodology of analysis for seismic design in different ductility classes according to Eurocode 8 (in the following EC8). The results obtained for an examined archetype Reinforced Concrete building are compared with the conventional RSA-based design to check pros and cons of LTHA as routine analysis methodology for “force-based” design. LTHA record selection is made according to EC8 consolidated practice for spectrum compatible accelerograms [8]. The archetype structure considered is a 12-storey moment resisting frame (MRF) allowing a reasonably significant effect of higher modes for the regular structure considered. A distinguishing aspect of the archetype structure designed is to include the staircase made with knee-beams, whose effect is often discarded in this kind of studies but it makes the design realistic and it reflects the engineering practice in Europe. Each relevant aspect of the design procedure according to EC8 has been considered and critically adapted to the employment of LTHA (e.g., reduction of the spectrum through behaviour factor, P-Delta effects).

Comparison of design results provide a proof of concept for the LTHA as explicit design method in EC8. On the other hand, critical aspects such as including accidental eccentricity, or controlling the variability of the input/results should be looked into more details in further studies.

## 2. Conventional EC8-Design of RC-MRF through RSA

The archetype building is a 12-storey RC-MRF designed according to EC8 [1] and EC2 [9], including specifications of the Italian National Annexes. In particular, two seismic designs are considered for the same building geometry; (i) Ductility Class High (DCH) design and (ii) Ductility Class Medium (DCM).

The building has 25x15 m<sup>2</sup> floor area used for office activities. Interstorey heights are 3.6 m and 3.0 m at first level and upper levels, respectively. Bay length is 5.0 m in both longitudinal (X) and transverse (Y) directions. The connection between floors is realized by means of staircase with knee beams and cantilever steps, commonly used in Italian building practice (see Fig. 1a).

The building is located in Pettino, neighbourhood of L'Aquila (Italy), having longitude 13°34'38.90"E and latitude 42°37'72.20"N. The area was significantly affected by the M6.3 2009 L'Aquila earthquake. Soil class B is assumed for the seismic actions characterization on the basis of information provided by the accelerometric stations located in the same area. The archetype building, in both ductility classes, is designed on the basis of structural simplicity, uniformity and symmetry criteria in order to obtain a clear and predictable transmission of the seismic forces. Section sizes of structural members are initially obtained by preliminary dimensioning on gravity loads and then modified on the basis of the seismic demand.

One-way slabs are made of RC joists and hollow blocks having width respectively equal to 10 cm and 40 cm. Joists' directions are chosen in order to uniformly distribute floor loads to the beams. A concrete slab of 4 cm is present to each floor in order to have sufficient in-plane stiffness for the distribution of horizontal inertia forces to the frames. Slabs' height is 20 cm (including roof level), equal to 1/25 of beam spans. Floor imposed load is 2.0 KN/m<sup>2</sup> (i.e., cat. B1, considering office destination). Roof imposed load is 0.50 KN/m<sup>2</sup> (i.e., cat. H, considering normal maintenance and repair access). Moreover, due to L'Aquila location, a snow load equal to 1.40 KN/m<sup>2</sup> is considered on the roof surface ( $a_s = 750$  m.a.s.l.).

The staircase is arranged centrally and adjacent to the longitudinal building facade, in order to satisfy both architectural and structural symmetry requirements. It consists of inclined beams connected by horizontal beams in correspondence of landing and floor levels (also known as "knee beam"). Steps are considered to have a structural function and they are fixed to the inclined beams as cantilever beams. Staircases are areas susceptible to crowding; thus, an imposed load for cat. C2, equal to 4.0 KN/m<sup>2</sup>, is assumed. The lift is placed in the stairwell and it is considered disconnected from the main structure. Perimeter infills are constituted by double layer hollow clay bricks. They are considered in the model as non-structural elements, realised in contact with the frame, without any structural connection with it.

Cross-sections of beams are assigned on the basis of values typically assumed in the constructional practice. Columns are designed in order to sustain an appropriate internal axial force both for seismic and non-seismic conditions, and they have to provide an adequate lateral stiffness to the structure. In addition, column cross-sections are assumed in order to achieve smoothly beam-to-column hierarchy (i.e., capacity design). Square cross-sections for all the columns are assumed allowing an equal distribution of lateral strength and stiffness in the two directions. Maximum columns' decrease at adjacent levels is 10 cm for reasons of regularity in elevation and constructional practice. Elastic flexural and shear stiffness properties of beams and columns in the model are 50% of uncracked gross section stiffness for both ultimate and serviceability limit states, in accordance with EC8 prescription.

According to the Italian National Annex, the design spectra in this study are obtained for two limit states (Fig. 1b): (i) Damage Limitation Limit State (DL-elastic), i.e., the elastic spectrum with 63% probability of exceedance 50 years, corresponding to a return period ( $T_R$ ) of 50 years; (ii) Life Safety Limit State (LS), assuming two behaviour factors ( $q$ ) equal to 5.85 and 3.90 for DCH and DCM, respectively, and based on the elastic spectrum with 10% probability of exceedance of 50 years ( $T_R = 475$  years).

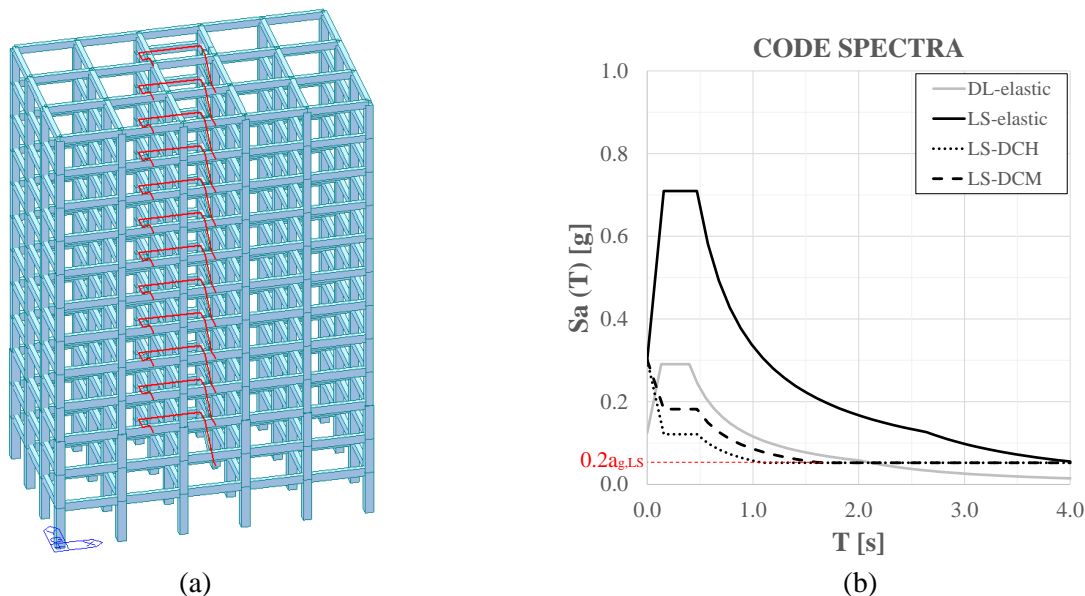


Fig. 1 – (a) Structural model of the archetype structure with staircase beams in red [10]; (b) Elastic spectra for Life Safety (LS-elastic) and Damage Limitation (DL-elastic), and LS design spectra for DCH and DCM.



DL capacity is based on the maximum Interstorey Drift Ratio (IDR) in compliance with damage limitation of non-structural elements, and it is equal to 5‰ according to EC8. DL demand is evaluated assuming the DL-elastic spectrum as seismic input. LS demand is evaluated assuming different  $q$  on the basis of ductility target. The archetype building is regular in plan and elevation, thus for DCH  $q = 5.85$ , while for DCM  $q = 3.90$ . The regularity of the structural configuration is still valid for the assumed symmetrical infills arrangement.

It is worth noting that the design spectra corresponding for both DCH and DCM are modified from  $T > 1.10$ s and  $T > 1.61$ s in order to consider the lower bound design value for the pseudo-acceleration imposed by EC8 ( $S_{ad}(T) \geq 0.2a_g$ ).

RSA for DCH and DCM design cases is performed through the commercial software package MIDAS Gen 2015 [10]. This software is chosen for its widespread use for professional applications and its adaptability to the case of LTHA (as discussed in section 4).

In the RSA method, the peak value  $E_{io}$  of the  $i^{\text{th}}$ -mode contribution to the seismic response is obtained from the design spectrum, see Eq. (1).  $E_{io}$  is evaluated through the design pseudo-acceleration  $S_{ad}(T_i, \zeta_i)$  at the modal period  $T_i$ , for the assumed damping of the  $i^{\text{th}}$ -mode ( $\zeta_i$ ), and the modal static response ( $E_i^{st}$ ).  $E_i^{st}$  may be positive or negative, while  $S_{ad}(T_i, \zeta_i)$  is positive by definition.

Results from each mode are then combined through the Complete Quadratic Combination (CQC), see Eq. (2), assuming that the peak values of the modes contributions are achieved in the same time instant in which the maximum response in terms of pseudo-acceleration occurs.

$$E_{io} = E_i^{st} S_{ad}(T_i, \zeta_i) \quad i = 1, 2, \dots, n \quad (1)$$

$$E_o = \sqrt{\sum_{i=1}^n \sum_{j=1}^n \rho_{ij} E_{io} E_{jo}} \quad (2)$$

In Eq. (2),  $E_{io}$  and  $E_{jo}$  are the values of seismic action effects due to the vibration mode  $i$  and  $j$ , respectively, and  $\rho_{ij}$  is the correlation coefficient between  $i$  and  $j$  modes as per Eq. (3) [4], where  $\zeta_i$  and  $\zeta_j$  are respectively the viscous damping coefficients of the  $i$  and  $j$  mode and  $\beta_{ij} = T_j / T_i$ , being  $T_i$  and  $T_j$  the corresponding periods.  $\rho_{ij}$  varies between 0 and 1, and it is equal to 1 for  $i = j$ , decreasing rapidly as the periods are more distant, especially for  $\zeta = 0.05$  (typical value for civil engineering structures).

$$\rho_{ij} = \frac{8\sqrt{\zeta_i \zeta_j} (\beta_{ij} \zeta_i + \zeta_j) \beta_{ij}^{3/2}}{(1 - \beta_{ij}^2)^2 + 4\zeta_i \zeta_j \beta_{ij} (1 + \beta_{ij}^2) + 4(\zeta_i^2 + \zeta_j^2) \beta_{ij}^2} \quad (3)$$

Eq. (2) produces internal forces and displacements as absolute values, thus the signs of the principal translational modes of vibration for the two main directions are then assigned to them. According to EC8, all the modes of vibration up to a cumulative effective modal mass of at least 90%, with an effective modal mass greater than 5% of the total mass have to be considered in the CQC.

In this preliminary feasibility study for LTHA, the effect of the accidental eccentricity of the centre of mass ( $e_{ai} = \pm 0.05 L_i$ ) is not taken into account in the analyses and only the spatial variation of the seismic motion (100:30 combination rule) is considered. For RSA, the application of the two rules result in 32 combinations of the seismic static forces in the main directions, while the only 30% combination rule results in 8 combinations.

Accidental eccentricity cannot be applied in LTHA in the same way as RSA, since it doesn't produce the same effect; in fact, the shift of the centre of mass changes the dynamic characteristics of the structure [11]. However, several procedures have been proposed to account for the effects of torsional ground motion in time history analyses [12], and they will be the object of further bespoke studies. At this stage, they are beyond the scope of this study.

## 2.1. DCH building design

Concrete C35/45 is adopted for the whole building in order to control section dimensioning because of beam-column joint verifications. The minimum cross-section area is 70x70 cm<sup>2</sup> for all the columns at the lower storeys. It results from the limitation on the normalized axial force ( $v_d \leq 0.55$ ). Beam-to-column joint verifications for



horizontal shear is the limiting design factor in DCH; it applies especially for the staircase joints and external joints at the upper storeys, where the internal axial compressive force is smaller. The minimum column cross-section area is 60x60 cm<sup>2</sup>, and it is adopted for all the columns at the upper storeys (see Fig. 2a).

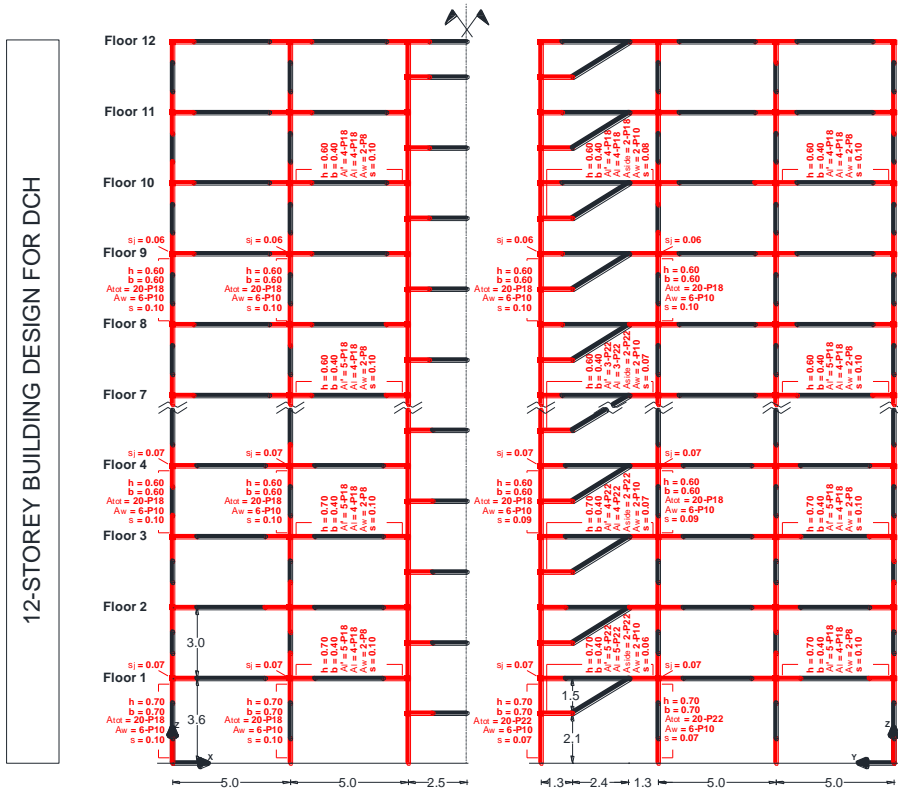
According to EC8, second-order effects (P-Δ) are taken into account for the entire structure by multiplying *a posteriori* all first-order action effects due to horizontal components of the seismic action by  $1/(1 - \vartheta_{max}) = 1.16$ , where  $\vartheta_{max}$  is the greatest of the values evaluated according to Eq. (4) for each direction [13]. For DCH design,  $\vartheta_{max}$  is equal to 0.14.

$$\vartheta_i = \frac{N_{tot,i} d_{r,i}}{V_{tot,i} h_i} \quad (4)$$

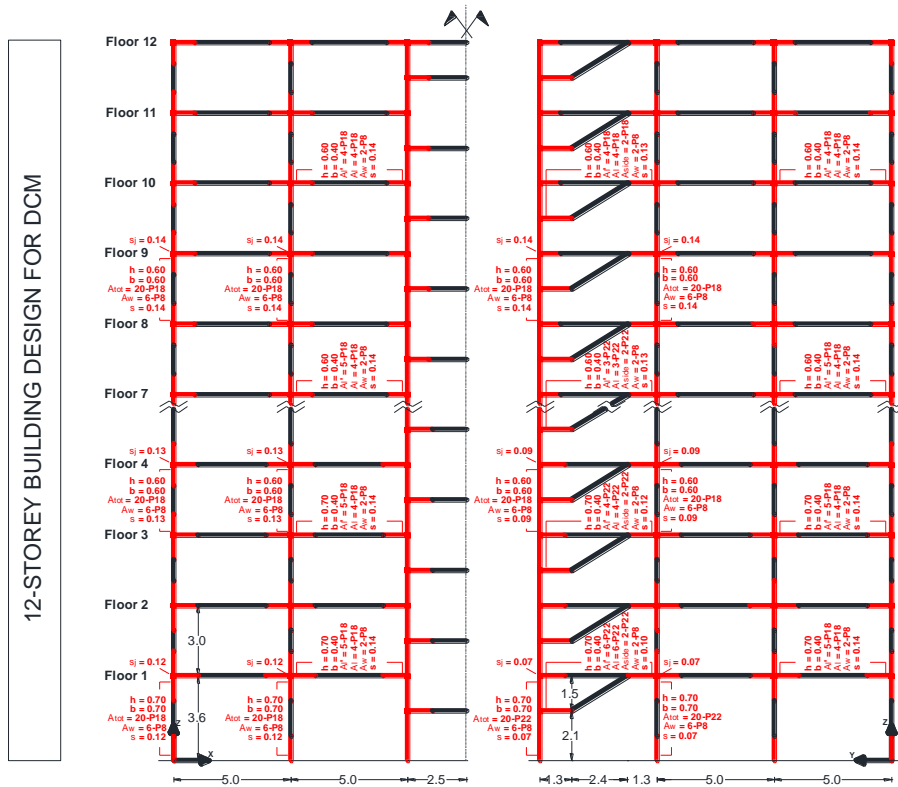
In Eq. (4),  $\vartheta_i$  is the interstorey drift sensitivity coefficient at  $i^{\text{th}}$ -storey.  $N_{tot,i}$  is the total gravity load concurrent with the seismic action at and above  $i^{\text{th}}$ -storey,  $d_{r,i}$  is the inelastic interstorey drift at the floor centre of mass, estimated via equal displacement rule (obtained multiplying the displacement by  $q$ ), finally,  $V_{tot,i}$  is the total seismic shear at  $i^{\text{th}}$ -storey, and  $h_i$  is the height of  $i^{\text{th}}$ -storey. The minimum number of the longitudinal bars into columns is imposed by the distance between consecutive bars restrained by horizontal hoops ( $\leq 150$  mm) and unrestrained bar from nearest restrained bar ( $\leq 150$  mm). The diameter of the longitudinal bars is increased to 22 mm only for staircase columns in order to satisfy the beam-column capacity design verification.  $\gamma_{Rd}$  is 1.2 and 1.3 when calculating shear force demands for beams and columns, respectively. Stirrup spacing ( $s$ ) in critical regions of beams is always limited by the longitudinal bars' diameter ( $s \leq 6d_{bL}$ ). The only exceptions are the knee beams in the staircase, for which  $s$  results from the truss capacity model with the inclination of the compression strut at 45 degrees. Stirrups' diameter is 10 mm in critical regions of all the columns in order to satisfy joint verification with feasible distances between hoops. Stirrup spacing in the critical regions of columns is generally governed by the minimum value equal to  $6d_{bL}$ , except for columns in the staircase where the critical condition is that on confinement imposing the minimum value for ductility compliance. Longitudinal and transversal reinforcement details of beams and columns are summarized in Fig. 2a.  $h$  and  $b$  are sections' depth and width,  $A_b$  and  $A_t$  are bottom and top longitudinal bars' area,  $A_{tot}$  and  $A_{side}$  are total and lateral total longitudinal bars' area,  $A_w$  is the transversal reinforcement area,  $s$  and  $s_j$  are the stirrup spacing in the elements and at the joint, respectively. Finally, DL limit state is checked. The maximum IDR attained in the building under the DL elastic spectrum (see Fig. 1b) is equal to 2‰; largely within the 5‰ capacity limit.

## 2.2. DCM building design

The seismic design of the building for DCM is made on the basis of the same concrete class (C35/45) and cross-sections' dimensions as obtained for DCH design. The same dimensioning is sufficient to satisfy the less restricting normalized axial force limit ( $v_d \leq 0.65$ ) of DCM according to EC8. No second-order effects amplification has to be considered in this case since  $\vartheta_{max}$  is lower than 0.10. Minimum number of longitudinal bars in the columns results from the minimum distance between consecutive restrained bars ( $\leq 200$  mm) and unrestrained bar from the nearest restrained bar ( $\leq 150$  mm). The diameter of longitudinal bars is increased to 22 mm only for the staircase columns in order to satisfy the beams-columns capacity design for these elements.  $\gamma_{Rd}$  is 1.0 and 1.1 when calculating shear force demands for beams and columns, respectively.  $s$  in beams' critical regions is always governed by the minimum value equal to  $8d_{bL}$ , except for the staircase beams, for which the minimum distance between stirrups is that resulting from the truss capacity model. The distance between stirrups in the critical regions of columns is governed by the confinement verification for ductility compliance at the lower storeys and the minimum value equal to  $8d_{bL}$  at the upper storeys. Stirrup spacing in beam-to-column joints is assumed to be the same of the corresponding bottom columns, although for confined central joints the spacing  $s_j$  can be doubled, being not greater than 150 mm. Reinforcement details of beams and columns for DCM design are respectively summarized in Fig. 2b. DL verification is exactly the same for DCH and DCM design since structure stiffness is the same for the two cases, being section dimensions the same.



(a)



(b)

Fig. 2 – Geometrical and reinforcement details for (a) DCH and (b) DCM.

Modal properties of the archetype structure are summarized in Table 1; i.e. periods ( $T$ ) and participating masses of the first ten modes are shown. These are the modes employed in the RSA and complying with the 90% rule on modal masses summation and 5% minimum on modes to be considered. The RSA is performed assuming conventional 5% damping for all the modes resulting in the correlation coefficients  $\rho_{ij}$  matrix as shown in Fig. 3. It is relevant how  $T_i$  and  $T_j$  for the 2<sup>nd</sup> and 3<sup>rd</sup> modes are really close, resulting in  $\rho_{23}$  equal to 1.

Table 1 – Summary of modal properties.

MODE	1 <sup>st</sup>	2 <sup>nd</sup>	3 <sup>th</sup>	4 <sup>th</sup>	5 <sup>th</sup>	6 <sup>th</sup>	7 <sup>th</sup>	8 <sup>th</sup>	9 <sup>th</sup>	10 <sup>th</sup>
T [s]	1.365	1.257	1.256	0.483	0.445	0.430	0.276	0.255	0.241	0.194
MASS-X [%]	77.3	0.6	0.0	12.0	0.1	0.0	4.2	0.0	0.0	2.2
MASS-Y [%]	0.0	5.3	71.0	0.0	0.0	13.8	0.0	0.0	4.4	0.0
ROTN-Z [%]	0.6	72.1	5.3	0.1	11.9	0.0	0.0	4.3	0.0	0.0

$$[\rho_{ij}] = \begin{bmatrix} 1.000 & 0.596 & 0.587 & 0.007 & 0.006 & 0.006 & 0.002 & 0.002 & 0.002 & 0.001 \\ & 1.000 & 1.000 & 0.009 & 0.007 & 0.007 & 0.003 & 0.002 & 0.002 & 0.001 \\ & & 1.000 & 0.009 & 0.007 & 0.007 & 0.003 & 0.002 & 0.002 & 0.001 \\ & & & 1.000 & 0.594 & 0.420 & 0.029 & 0.022 & 0.018 & 0.010 \\ & & & & 1.000 & 0.892 & 0.040 & 0.030 & 0.024 & 0.012 \\ & & & & & 1.000 & 0.046 & 0.034 & 0.027 & 0.014 \\ & & & & & & 1.000 & 0.628 & 0.348 & 0.073 \\ & & & & & & & 1.000 & 0.737 & 0.115 \\ & & & & & & & & 1.000 & 0.175 \\ & & & & & & & & & 1.000 \end{bmatrix}$$

*sym*

Fig. 3 – Correlation matrix for  $\rho_{ij}$  coefficients evaluated for the first ten modes of the building referred to periods  $T_i$  in Table 1 and relative damping  $\xi_i$  equal to 5% for all the modes.

### 3. LTHA as design method

The same buildings previously designed for DCH and DCM through RSA are here analysed considering LTHA's results for two sets of accelerograms for each limit states considered. RSA can directly determine the exact peak response of Single-Degree-of-Freedom (SDOF) systems without carrying out a LTHA but the results of the two analyses are different for Multiple-Degree-of-Freedom (MDOF) systems [14]. LTHA, strictly speaking, is an analysis applied to a linear model of the structure in which the input is characterized by accelerometric waveforms resulting by seismic input selection, based on hazard analysis at the site. Herein, it is discussed how and to what extent the force-based EC8 design procedure through RSA (as described in the previous section) can be adapted for the more accurate LTHA.

The primary benefit LTHA is that it considers the interaction of the modes of vibration with the typical frequencies of an earthquake defined by accelerometric waveforms. From the mathematical point of view, the differential equations that govern the seismic response of a discrete linear  $n$ -degree of freedom structure with  $[M]$ ,  $[C]$ , and  $[K]$ , mass, damping and stiffness matrices, can be expressed as shown in Eq. (5), where  $\{\ddot{u}(t)\}$  is the relative acceleration vector,  $\{\dot{u}(t)\}$  is the relative velocity vector,  $\{u(t)\}$  is the relative displacement vector,  $\{\tau\}$  is the influence coefficient vector and  $\{\ddot{u}_g(t)\}$  is the earthquake-induced ground motion acceleration. The solution of Eq. (5) is based on decoupling concepts and orthonormality mode of vibration, which both allow to solve  $n$ -responses of SDOF systems

$$[M]\{\ddot{u}(t)\} + [C]\{\dot{u}(t)\} + [K]\{u(t)\} = -[M]\{\tau\}\{\ddot{u}_g(t)\} \quad (5)$$

Unlike RSA, which provides a snapshot of the peak condition, LTHA provides the structural response  $E(t)$  as a function of time, accounting for the whole duration of the earthquake. In this way, LTHA can distinguish impulsive earthquakes (characterized by a strong energy dissipation in one or few pulses without reversal sign) and sinusoidal earthquakes (in which the energy dissipation occurs in many cycles with many sign inversions). It is clear that the analysis is performed on a linear model, thus energy dissipation due to hysteretic effects cannot be captured and only that related to viscous damping can. Furthermore, the full time-history can overpass known limitations of CQC and the problem of sign assumption in RSA. For the purposes of this work, the maximum values of the response (internal forces, storey shears and displacements) are compared for the RSA versus LTHA applied to the archetype building when designed for DCH and DCM.

### 3.1. EC8 compliant record selection

The implementation of LTHA requests for a conventional procedure. In the following, we start from record selection and we discuss "force-based" LTHA up to the final design verifications for EC8-compliant structures. According to EC8, the seismic motion can be real, artificial or simulated. Nowadays, real accelerograms are easily available from most common ground motion databases, and they are also preferable compared to others, thanks to the real frequency content, the correct time correlation between the components and the realistic energetic content referred to seismological parameters. Every set of accelerograms should be formed by at least seven different couples of records in order to consider the mean results of the analysis for all the response quantities as design values in the relevant verifications. Since the same accelerogram may not be used simultaneously along both horizontal directions, by swapping the pairs of horizontal records in the main directions of the considered structure, the number of the analysis becomes 14. For the sake of simplicity, the vertical component of the seismic action is not considered in the analyses, but it can be neglected for the examined type of structure. The accelerograms used in the time-history analyses are selected through the Matlab-based software REXEL [8]. In particular, 7 pairs of unscaled real records from the European Strong Motion Database are obtained from REXEL for both LS and DL. Records for the two limit states are spectrum-compatible with the elastic spectra. They are selected so that the mean spectra match the smoothed Newmark-Hall shape code between 10% lower and 30% upper tolerances in the period range of 0-4s. EC8, for nonlinear time-history analyses, asks for compatibility up to  $2T_l$ , but the compatibility for the LTHA has to be guaranteed up to  $T_l$ , being the analysis linear. Disaggregation of seismic hazard is performed for  $S_a(I_s)$ , and respectively for magnitude and source-to-site distance intervals of M4.5-7.5 and 0-30 km. Selection results for both LS and DL are shown in Fig. 5a and 5b, respectively.

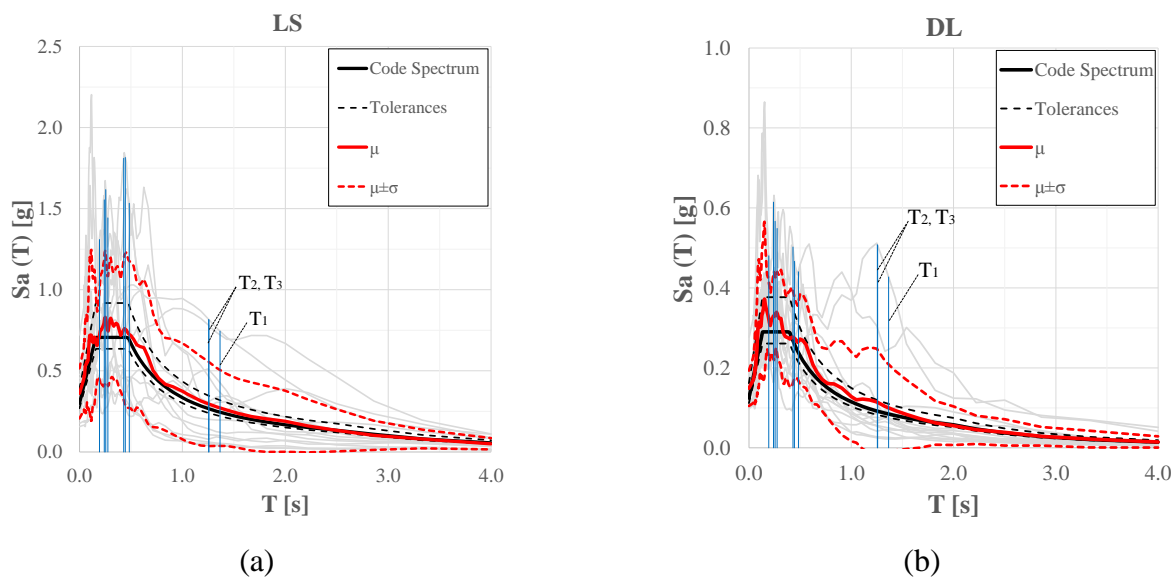


Fig. 5 – Sets of 7 couples of spectrum-compatible accelerograms with (a) LS-elastic and (b) DL-elastic smooth code spectra.

Once records sets are selected for the two limit states, for DL the accelerograms are considered as input, while for LS the records are divided by  $q$ . From mathematical point of view, this scaling is equivalent to a spectral matching with the design spectra, unless for the branch  $0 \leq T \leq T_B$  where the design spectrum equation is not linearly reduced by  $1/q$ . Moreover, in order to account for the imposed lower bound value of the pseudo-acceleration ( $S_a(T) \geq 0.2a_g$ ), a new rule is here assumed for the behaviour factor to be applied to accelerograms as shown in Eq. (6).  $S_{ae}(T_i)$  and  $S_{ad}(T_i)$  are respectively the values of the spectral acceleration corresponding to  $T_i$  evaluated on the elastic and design smoothed spectra. In the analysed cases, the introduced rule only affects the value of the scaling factor  $1/q$  for DCH, which is equal to  $1/4.65$  instead of  $1/5.85$  due to the  $0.2a_g$  limitation affecting the design spectrum in a period range included in the interval  $[T_B, T_I]$ , being  $T_I=1.365s$ .

$$q_{LTHA} = \min \left[ \frac{S_{ae}(T_i)}{S_{ad}(T_i)} \right]_i \quad \forall T_B \leq T_i \leq T_I \quad (6)$$

#### 4. Results and comparison with RSA

Comparison between RSA and LTHA at LS limit state for DCH shows mean relative errors ( $e_{(LTHA-RSA)/RSA}$ ) in terms of storey shears (SS) of +19% and +25% for X and Y direction, respectively (see Fig. 6a, 6b and 8a). For DCH, LTHA design is performed with a scaling factor of the acceleration equal to  $1/4.65$ , from Eq. (6), and accounting for second-order effects (P- $\Delta$ ), according to EC8, with an amplification factor of the acceleration equal to 1.16. In fact, the approximate procedure to compute  $\vartheta_{max}$  can be applied in the same way to LTHA. Demand differences are mostly attributable to the spectral accelerations differences between code and mean spectra in correspondence to the main translational periods, equal to +11% for  $T_1$  and  $T_3$ . Beam design is different from 1<sup>st</sup> to 6<sup>th</sup> storey, where one more longitudinal bar is required at both the edges of sections in order to satisfy the maximum/minimum time-history flexural demand. Bottom and top geometric reinforcement ratio  $\rho_l$  and  $\rho_l'$  for these elements changes respectively from 0.39% and 0.48% to 0.48% and 0.58%. However, such increment did not lead to changes in beam transverse reinforcement. Columns' design has not changed; in fact, these elements were overdesigned due to the restrictive reinforcement detail rules on restrained bars.

Comparison between RSA and LTHA at LS limit state for DCM shows mean relative error in terms of base shear of +25% and +22% for X and Y direction, respectively (see Fig. 6c, 6d and 8b). LTHA design is performed with a scaling factor of the acceleration equal to  $1/3.90$ , from Eq. (6), and accounting for second-order effects (P- $\Delta$ ), according to EC8, with an amplification factor of the acceleration equal to 1.11.  $\vartheta_{max}$  for the DCM design is on the boundary and it has to be considered for LTHA and it can be neglected for RSA. Discarding the P- $\Delta$  amplification for LTHA, the mean error in terms of base shear would have been of +12% and +10%, comparable to the spectral accelerations differences between code and mean spectra in correspondence to the main translational periods. Such differences would have been similar for DCH design through RSA and LTHA designs without both the P- $\Delta$  amplification factor and  $0.2a_g$  lower limit of the pseudo-acceleration (i.e., the analysis is linear). For DCM case, beam design is different at 1<sup>st</sup> to 7<sup>th</sup> storey, and for staircase knee beams at the 3<sup>rd</sup> storey. In both cases, one more longitudinal bar is required at both the edges of sections in order to satisfy the maximum/minimum time-history flexural demand. The additional bar modify  $\rho_l$  and  $\rho_l'$  for these elements respectively from 0.39% and 0.48% to 0.48% and 0.58%, and total geometric reinforcement ratio  $\rho_{tot}$  of the knee beams from 1.63% to 1.90%. The diameter of the longitudinal bars is increased to 22 mm only for the staircase columns from 4<sup>th</sup> to 8<sup>th</sup> storey in order to satisfy the beams-columns capacity design, ending up to the same bar dimensions of lower storeys.

For DL limit state (verification and analysis are the same for both DCH and DCM), the mean relative errors is +10% and +17% in terms of top displacement in X and Y direction, respectively (see Fig. 7a and 7b). For the DL case, the gap between code and arithmetically averaged spectra in correspondence to the main translational periods is equal to +18% and +24% for  $T_1$  and  $T_3$ , respectively. Relative error in terms of displacements is approximately constant and equal to 16%; Mean relative error in terms of IDR varies from +32% (at 12<sup>th</sup> storey) to +22% (8<sup>th</sup> storey) in X and Y direction (see Fig. 8c). Maximum D/C for DL is 0.40 for RSA, and it becomes 0.43 for LTHA in X direction and 0.35 and 0.42 for Y direction (attained between 3<sup>rd</sup> and 4<sup>th</sup> storey in all cases).

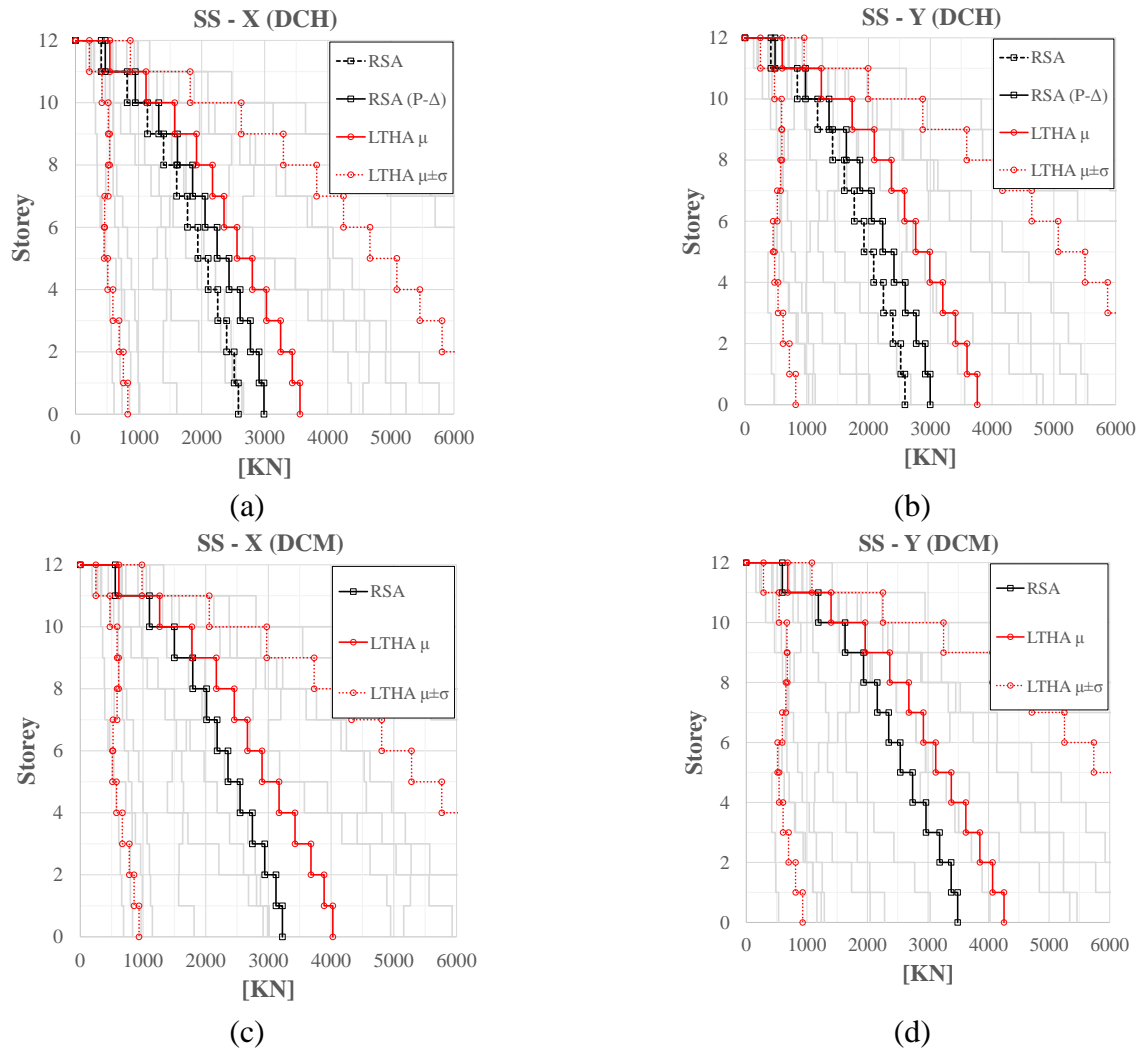


Fig. 6 – Mean ( $\mu$ )  $\pm$  one standard deviation ( $\sigma$ ) for envelope of Storey Shears (SS) in the case of LTHA (red) compared with RSA (black) at LS for DCH in (a) X and (b) Y, and DCM for (c) X and (d) Y directions.

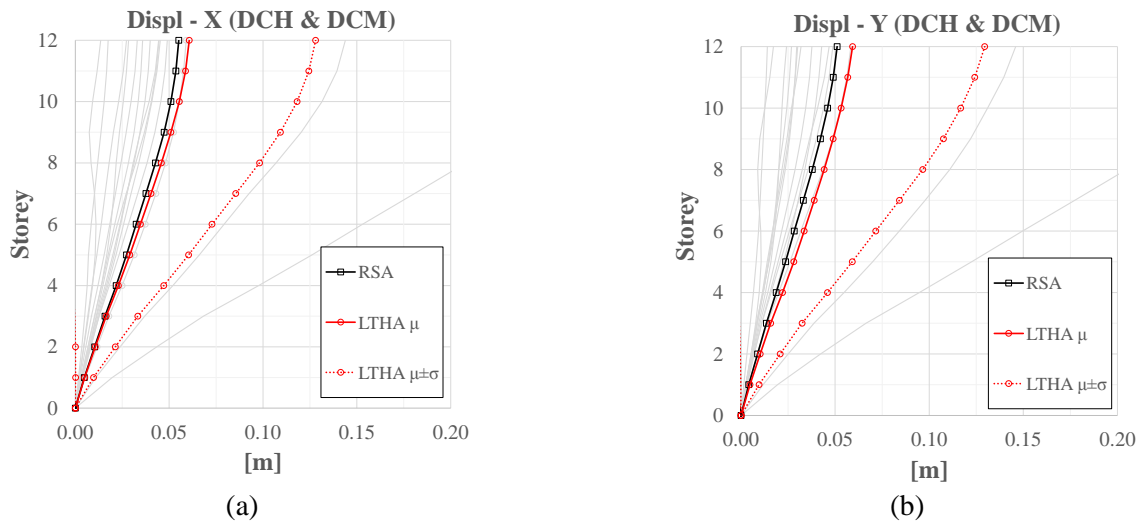


Fig. 7 – Mean ( $\mu$ )  $\pm$  one standard deviation ( $\sigma$ ) for envelope of Displacements (Displ) in the case of LTHA (red) compared with RSA (black) at DL in (a) X and (b) Y directions (same results for DCH and DCM).

Coefficient of Variation ( $CoV$ ) for SS and IDR at each storey, i.e., the ratio of the standard deviation ( $\sigma$ ) to the average ( $\mu$ ), for LS and DL limit states are shown in Table 2. Note that  $CoV$  for SS at each storey are the same for DCH and DCM. SS and IDR's  $CoVs$  can be compared to those of the elastic spectral ordinates of the 14 records in each of the two sets for LS and DL at the two fundamental translational periods of the structures ( $T_1$  and  $T_3$ ). Comparison of SS and IDR  $CoVs$  with that of  $S_a(T_1)$  and  $S_a(T_3)$  provides a quantitative indication of higher mode response in LTHA and insight on how the input should be controlled at the fundamental period for practical design application. In this case,  $COV_{S_a(T_1)}$  and  $COV_{S_a(T_3)}$  are 0.86 and 0.88 for the LS set of records and 1.09 and 1.15 for the DL set of records.

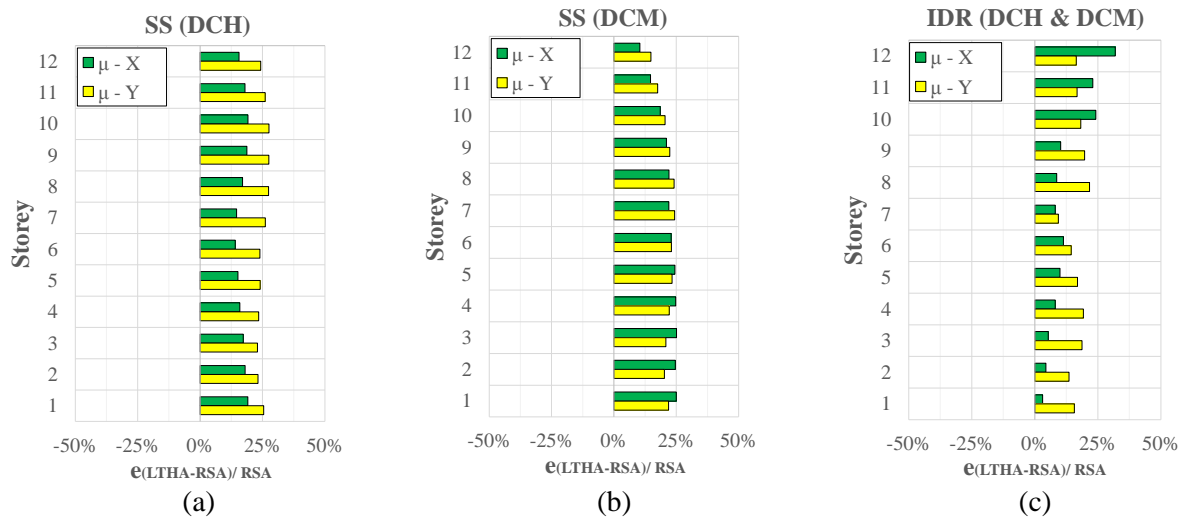


Fig. 8 – Relative errors between LTHA and RSA for Storey Shears (SS) at LS limit state for (a) DCH and (b) DCM design and (c) for Interstorey Drift Ratios (IDR) at DL limit state in X and Y directions (green and yellow).

Table 2.  $CoV$  of SS and IDR for X and Y direction at each storey LS (DCH design) and DL limit states.

	STOREY	1 <sup>st</sup>	2 <sup>nd</sup>	3 <sup>rd</sup>	4 <sup>th</sup>	5 <sup>th</sup>	6 <sup>th</sup>	7 <sup>th</sup>	8 <sup>th</sup>	9 <sup>th</sup>	10 <sup>th</sup>	11 <sup>th</sup>	12 <sup>th</sup>
LS	$CoV_{SSi,X}$	0.77	0.78	0.79	0.80	0.82	0.82	0.80	0.76	0.72	0.67	0.62	0.59
	$CoV_{SSi,Y}$	0.78	0.80	0.82	0.83	0.84	0.84	0.80	0.75	0.71	0.66	0.61	0.58
DL	$CoV_{IDRi,X}$	0.97	1.01	1.06	1.14	1.19	1.20	1.26	1.30	1.20	1.00	0.91	0.85
	$CoV_{IDRi,Y}$	1.03	1.05	1.09	1.14	1.21	1.28	1.36	1.37	1.28	1.20	1.13	1.07

## 5. Conclusions and future challenges

Linear Time-History Analysis (LTHA) is discussed as alternative force-based design method to conventional Response Spectrum Analysis (RSA) for possible explicit inclusion in Eurocode 8. In order to investigate on possible relevant differences, an archetype 12-storey regular Reinforced Concrete Moment Resisting Frame is designed in Ductility Class High and Medium according to Eurocode 8. After a conventional RSA design is performed, two sets of fourteen spectrum compatible accelerograms are selected (based on the consolidated practice for Eurocode 8-compliant record selection).

LTHA methodology with mean results (median should be investigated in future) is always on the safe-side for the design of the archetype with respect to RSA. Differences between the two methodologies can achieve a +25% in terms of forces for the examined regular archetype structure and for the considered selection of records. Aspects like the best rule for the application of the behaviour factor to the accelerograms, or consideration of P-Delta effects are considered herein and solved on the basis of typical practice of either RSA or Nonlinear Time-History Analysis. Interstorey drift ratio verification did not influence the design of the examined archetype building



due to the assumption of large cross-section to satisfy the beam-to-column joints verifications. However, the difference between the two analyses can achieve at upper storeys a +32% for the examined structure in terms of displacements.

The archetype structure is regular and, at this stage, accidental eccentricity was neglected in both RSA and LTHA, since a bespoke procedure has to be tested in future for LTHA. The comparison between LTHA and RSA needs to be generalized for different types of structures (irregular and stiffer to emphasize the advantages of LTHA where complete quadratic combination has problems) and with a greater number of records to provide robust suggestions on control of standard deviation for record selection.

Linear Time-History Analysis has also a great potential as methodology for the assessment of approximate fragility curves for intermediate level of damage (excluding collapse), serviceability limit states and for bespoke analyses for near source conditions. The target is to come up with a robust methodological procedure both force-based and displacement-based to promote this method as option in future versions of Eurocode 8.

## 6. Acknowledgements

The authors wish to acknowledge the Alumni Foundation of University of Bristol for the support provided to Luca Lombardi to attend the 16WCEE conference in Santiago (Chile).

## 7. References

- [1] EN 1998-1 Eurocode 8 (2004): Design of structures for earthquake resistance – Part 1: General rules, seismic actions and rules for buildings, European Committee for Standardization (CEN), Brussels, BE.
- [2] Rosenblueth E (1951): A basis for aseismic design. PhD thesis, University of Illinois, Urbana, Ill.
- [3] Wilson EL, Der Kiureghian A, Bayo EP (1981): A replacement for the SRSS method in seismic analysis. *Earthquake Engineering and Structural Dynamics*, **9**, 187-192.
- [4] Der Kiureghian A (1981): A response spectrum method for random vibration analysis of MDF systems. *Earthquake Engineering and Structural Dynamics*, **9**, 419-435.
- [5] Gupta AK (1990): Response spectrum method in seismic analysis and design of structures. Blackwell, Cambridge, Mass.
- [6] De Luca F, Verderame GM (2013): The accuracy of CQC and response spectrum analysis in the case of impulsive earthquakes. *Proceedings of the 11<sup>th</sup> International Conference on Structural Safety and Reliability ICOSSAR 2013*, New York, USA.
- [7] Cacciola P, Colajanni P, Muscolino G (2004): Combination of Modal Responses Consistent with Seismic Input Representation. *Journal of Structural Engineering*, ASCE, **130**: 47-55.
- [8] Iervolino I, Galasso C, Cosenza E (2010): REXEL: computer aided record selection for code-based seismic structural analysis. *Bull. Earthquake Eng.*, **8**, 339-362.
- [9] EN 1992-1-1 Eurocode 2 (2004): Design of concrete structures – Part 1-1: General rules and rules for buildings, *European Committee for Standardization* (CEN), Brussels, BE.
- [10] SINCE (1989): MIDAS Information Technology Co., Ltd.
- [11] De La Llera JC, Chopra AK (1994): Accidental torsion in buildings due to base rotational excitation. *Earthquake Engineering and Structural Dynamics*, **23**, 1003-1021.
- [12] Basu D, Constantinou MC, Whittaker A (2014): An equivalent accidental eccentricity to account for the effects of torsional ground motion on structures. *Engineering Structures*, **69**, 1-11.
- [13] Fardis MN (2009): Seismic Design, Assessment and Retrofitting of Concrete Buildings - Based on EN-Eurocode8. Springer Dordrecht Heidelberg London New York.
- [14] Chopra AK (2012): Dynamics of the Structures – Theory and Applications to Earthquake Engineering, 4<sup>th</sup> Ed Prentice Hall.